

# Comparative Study and Validation of Photovoltaic Model Formulations for the IBPSA Modelica Library based on Rooftop Measurement Data

Laura Maier<sup>1</sup> Christoph Nytsch-Geusen<sup>2</sup> Lucas Westermann<sup>2</sup> Kushagra Mathur<sup>2</sup>  
Michael Wetter<sup>3</sup> Dirk Müller<sup>1</sup>

<sup>1</sup>Institute for Energy Efficient Buildings and Indoor Climate, E.ON Energy Research Center, RWTH Aachen University, Germany, {laura.maier, dmuller}@eonerc.rwth-aachen.de

<sup>2</sup>Institute for Architecture and Urban Planning, Berlin University of the Arts, Germany, {nytsch, k.mathur}@udk-berlin.de

<sup>3</sup>Lawrence Berkeley National Laboratory, Berkeley CA, USA, mwetter@lbl.gov

## Abstract

Domain-overarching system models are crucial to investigate sector coupling concepts. Specifically, the coupling of building and electrical energy systems becomes crucial to integrate renewable energy sources such as photovoltaic power systems (PV). For such interdisciplinary models, Modelica is a suitable language. However, most open-source Modelica libraries are either domain-specific or lack simple-to-parameterize PV models. We close this gap by developing a PV model for the IBPSA Modelica Library. The model comprises two I-V-characteristic models and three mounting-dependent cell temperature models. The I-V-characteristic models follow a single- and two-diodes approach. This study uses measurement data from a rooftop PV system in Berlin, Germany, for validation. The focus lies on comparing the implemented single- and two-diodes approach. Results prove that both models accurately calculate the modules' DC power output and cell temperature.

*Keywords: PV, Modelica, Validation, Open-Source*

## 1 Introduction

Interconnected systems facilitate the integration of renewable energy sources resulting in a decrease in  $CO_2$  emissions. One important sector with a high emission reduction potential is the building sector (2022 *Global status report for buildings and construction: Towards a zero-emissions, efficient and resilient buildings and construction sector* 2022). The electrification of buildings' energy systems has proven to be a valuable instrument to integrate renewable energy sources from the grid and, hence, interconnect sectors. Consequently, synergy effects arise from the connection of the two sectors while the system complexity increases. Buildings cannot only exploit renewable energy sources from the distribution grid level but also make use of self-generated electricity by, e.g., photovoltaic power plants (PV). PV is already a common way in practice to integrate renewable energy sources on both

a small and large scale. Exemplary PV application fields in the building sector are rooftop PV, facade-integrated PV, and stand-alone PV on district level. While designing building energy systems is already a challenge, it becomes even more complex when also considering potential PV integrations. Here, simulation tools support the design and operation of such interconnected systems.

For building energy systems, Modelica has proven to be a suitable modeling language. In this regard, open-source libraries facilitate the knowledge transfer from research to practice and harmonize the modeling process. As an outcome of the Annex 60 project and the subsequent Project 1 (Wetter, Treeck, et al. 2019), five modeling libraries focusing on building performance simulations started their collaboration. Among the five modeling libraries are one core library and four derivative libraries. The four derivative libraries, namely Buildings (Wetter, Zuo, et al. 2014), BuildingSystems (Nytsch-Geusen, Huber, Ljubijankic, et al. 2013), IDEAS (Jorissen et al. 2018), and AixLib (Maier, Jansen, et al. 2023) share a common core library, called Modelica IBPSA Library. These libraries aim to provide models for all relevant domains in building energy systems, namely, HVAC components and subsystems, building envelope models as well as internal and external boundary conditions. In addition, the derivative libraries partially include relevant electrical components, such as battery energy storage and PV models. However, prior to this development, the core library IBPSA neither includes an electrical package nor a PV model. Consequently, the derivative libraries have developed their own modeling approaches. This work aims at harmonizing the existing work by implementing a PV model in the core library.

The development is motivated by the already existing infrastructure between the core and its derivative libraries as well as the wide selection of building energy systems-related models and unified interfaces. We implement and compare two popular modeling approaches for PV systems, namely, the single- and two-diodes model approach.

While the former is an easy-to-parameterize and more simplified model, the latter is a more accurate representation of the physical behavior of the PV cell. Both models are compared and validated based on real measurement data from a rooftop PV system based on thin-film CIGS modules in Berlin, Germany.

## 2 Related work

This section gives an overview of existing modeling approaches for PV modules. At first, we define relevant criteria for the developed model. Subsequently, popular modeling approaches are discussed including their advantages and disadvantages. Following, existing Modelica models and libraries are presented.

### 2.1 Requirements

PV systems interact with building energy systems in various ways. While rooftop PV systems are the most common installation type in building energy systems, stand-alone PV systems play an important role in the context of district energy systems. Consequently, the focus lies on both PV system types. The present study does not focus on PV systems interacting with the thermal building mass, e.g., facade-integrated PV, despite their potential. In addition, this study aims at developing PV system models for the building design and operating phase focusing on energy performance. Consequently, the overall PV system's output power, rather than a detailed cell analysis, is the main performance metric. Since the models aim at supporting both practitioners and researchers, the parameterization effort should account for limited available information. In addition, the model execution time should be short so that different system configurations can quickly be assessed for annual system performance. To summarize, we define the following criteria for the model(s):

1. Representation of a rooftop or stand-alone PV system.
2. Suitability for energy performance evaluation.
3. Modular modeling approach for simple extensions and adaptations.
4. Simple parameterization based on readily accessible data.
5. Fast model execution for annual simulation.

### 2.2 Photovoltaic modeling approaches

The present study distinguishes the modeling approaches in electrical and thermal model. We first focus on the electrical modeling and discuss thermal models subsequently.

#### 2.2.1 Electrical modeling approaches: I-V characteristic

In the literature, there exist different approaches to model the electrical characteristics of a PV module, the so-called I-V-characteristic. These approaches can be distinguished into empirical and physics-based models. In the context of

this study, the latter are further differentiated into single- and two-diodes models, corresponding to the electrical equivalent circuit that they are based on. For the present study, we compare different techniques regarding their accuracy, computational effort, and parameterization effort. Table 1 shows a qualitative comparison based on the following literature review.

**Table 1.** Comparison of modeling techniques.

<i>Scheme</i>	<i>Accuracy</i>	<i>Comp. effort</i>	<i>Parameter.</i>
Empirical	+	+	-
Single-diode	0	+	+
Two-diodes	+	- to 0	0

#### Empirical approaches

Two well-known empirical PV modeling approaches are the Sandia PV Array Performance Model (SAPM) (King, Boyson, and Kratochvill 2005) and the Loss Factors Model (LFM) (Sellner et al. 2012; Sutterlueti et al. 2008). To obtain these models, selected points of the electrical characteristic, are determined based on measurement data. Those points cover the maximum power point (MPP), the short circuit current  $I_{sc}$  and the open-circuit voltage  $V_{oc}$ . In addition, fitting parameters are calculated based on measurement data that consider the change in the I-V characteristic with a change in irradiation and the cell temperature. Stein et al. (2013) and De Soto, Klein, and Beckman (2006) compare empirical models with numerical single-diode models. In these experiments, De Soto, Klein, and Beckman (2006) prove that the empirical models outperform the single-diode approach. Their explanation for this phenomena lies in a variety of experimental data that was used to fit the parameters of the empirical models.

#### Single-diode approach

In contrast to the empirical models, physics-based models are based on the assumption that PV cells can be described as diode circuits. Two approaches are common: The single- and the two-diodes approach (see Figure 1 and Figure 2). The single-diode model assumes that the PV modules' current  $I_{PV}$  can be described as the sum of the photo current  $I_{ph}$ , the leakage current  $I_{sh}$ , and the dark current  $I_d$  (see Figure 1).  $I_d$  is opposed to  $I_{ph}$ .  $I_d$  derives from the Shockley equation

$$I_d = I_s \left( e^{\frac{U+IR_s}{a}} - 1 \right), \quad (1)$$

where  $a$  denotes the modified ideality factor

$$a = \frac{N_s n_I k T_{cell}}{q}, \quad (2)$$

where  $I_d$  and  $a$  are based on the saturation current  $I_s$ , the ideality factor  $n_I$ , the elementary charge  $q$ , the Boltzmann constant  $k$ , and the cell temperature  $T_{cell}$ .  $R_s$  is the serial

resistance resulting in a voltage loss, while  $R_{sh}$  is the shunt resistance that leads to the leakage current  $I_{sh}$ . The result is the I-V characteristic

$$I = I_{ph} - I_d - I_{sh}, \quad (3)$$

$$I = I_{ph} - I_s \left( e^{\frac{U+IR_s}{a}} - 1 \right) - \frac{U + IR_s}{R_{sh}}. \quad (4)$$

These equations have five unknown parameters  $I_{ph}$ ,  $I_s$ ,  $a$ ,  $R_s$ , and  $R_{sh}$ , which is why they are referred to as 5p modeling approach. This approach is a compromise between accuracy, parameterization effort, and computational effort (see Table 1).

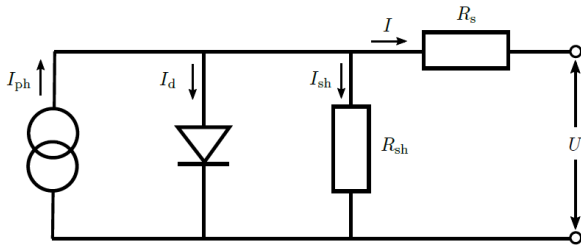


**Figure 1.** Single-diode equivalent circuit

The five parameters can be computed numerically or analytically. Both approaches are based on the idea that the five unknown parameters are calculated for standard conditions first and their change with changing operating conditions is computed subsequently. For more details, we refer to Duffie and Beckman (2013) for an exemplary numerical solution method and to E. I. Batzelis and Papatthanassiou (2015) for an analytical approach. The analytical approach's advantage over the numerical one lies in more robust and quick computation times (E. Batzelis 2019).

### Two-diodes approach

The two-diodes model is a refinement of the single-diode approach introducing a second diode into the electrical equivalent representation (see Figure 2).

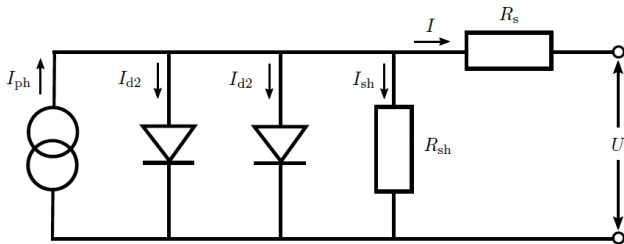


**Figure 2.** Two-diodes equivalent circuit

According to this model, the I-V characteristic of a PV module can be described as

$$0 = I_{ph} - I_{S1} \left( e^{\frac{U + \frac{I}{n_{par}} R_s}{U_t}} - 1 \right) - I_{S2} \left( e^{\frac{U + \frac{I}{n_{par}} R_s}{2U_t}} - 1 \right) - \frac{\frac{U}{n_{ser}} + \frac{I}{n_{par}} R_s}{R_{sh}} - \frac{I}{n_{par}}, \quad (5)$$

$$U_t = k \frac{T_{cell}}{e}, \quad (6)$$

$$I_{ph} = (c_1 + c_2 0.001 T_{cell}) H, \quad (7)$$

$$I_{S1} = c_{S1} T_{cell}^3 e^{-\frac{E_g}{k T_{cell}}}, \quad (8)$$

and

$$I_{S2} = c_{S2} \sqrt{T_{cell}^5} e^{-\frac{E_g}{2k T_{cell}}}. \quad (9)$$

These equations contain six parameters ( $R_s, R_{sh}, c_1, c_2, c_{S1}, c_{S2}$ ), which cannot be taken directly from the module manufacturer's data sheets. Instead, they must be obtained by parameter identification from the module's I-V characteristics for different module temperatures. Consequently, the two-diodes approach results in a high accuracy due to a detailed representation of the I-V characteristic, but it results in a higher computational effort due to an additional parameter fitting process and, hence, a more complicated parameterization.

### 2.2.2 Cell temperature calculation

The cell temperature affects the I-V characteristic and, hence, the electrical efficiency of the PV module. The absorbed irradiation is partially transformed into electrical and thermal energy within the cell. The module's heat transfer to the ambient is influenced by the wind velocity, the ambient temperature, and the irradiation. The energy balance can be formulated as

$$G_n(\tau\alpha) = \eta_c G_n + U_T(T_{cell} - T_{ambient}), \quad (10)$$

where  $\tau\alpha$  is the transmission-absorption coefficient of the module that accounts for the transmission of the glazing and the absorption of the anti-reflection layer,  $\eta_c$  is the cell efficiency under operating conditions and  $U_T$  the heat transfer coefficient (Duffie and Beckman 2013; Jakhрани et al. 2011). Duffie and Beckman (2013) and Jakhрани et al. (2011) describe that the energy balance can be solved using the normal operating cell temperature (NOCT) conditions that assume no load conditions, no wind, and a module tilt of  $45^\circ$  as

$$T_{cell} = T_{ambient} + (T_{NOCT} - 20^\circ\text{C}) \frac{G_n}{800 \text{ W/m}^2} \frac{U_{T,NOCT}}{U_T} \left( 1 - \frac{\eta_c}{(\tau\alpha)_{NOCT}} \right). \quad (11)$$

Because some parameters, such as  $(\tau\alpha)_{NOCT}$  and  $U_T$ , are difficult to assess, some studies neglect their influence by assuming no load conditions and no wind (Romary et al. 2011) or real operating conditions and no

wind (Bai et al. 2014). Other studies find empirical relations to consider the wind velocity's influence on the cell temperature (Duffie and Beckman 2013; Romary et al. 2011). Apart from the NOCT-based approaches, which are purely physical or a mix of empirical or physical models, there exist purely empirical approaches, such as described by King, Boyson, and Kratochvill (2005). King, Boyson, and Kratochvill (2005) develop empirical solutions for two different mounting types, i.e., a type with an installation close to ground and the other installed in contact with the ground.

### 2.3 Existing photovoltaic models in Modelica libraries

The following review investigates already existing open-source PV models in Modelica. We distinguish models that are part of the *Project I*-related derivative libraries from external libraries. All of the derivative libraries of the *IBPSA* core library contain some type of PV model. While the *AixLib* and *IDEAS* library both contain a model based on the 5p-modeling, i.e., single-diode approach (see subsection 3.1.2), the *Buildings* library contains two simplified models assuming constant efficiencies. The model implemented in the *AixLib* library contains different cell temperature models accounting for three mounting types (open rack, close to the ground, and in contact with the ground) following Duffie and Beckman (2013) and King, Boyson, and Kratochvill (2005). In contrast, the models implemented in the *IDEAS* library use a simplified approach for which a heat transfer coefficient needs to be known. Both models assume an internal MPP tracker. In contrast to that, the models implemented in the *BuildingSystems* library cover both single- and two-diodes models with and without internal MPP tracking (Pruthviraj Balekai 2018; Nytsch-Geusen, Huber, and Nie 2013).

In contrast to the *IBPSA*-related libraries, two specialized open-source libraries for PV system simulation exist: the *PhotoVoltaics* (Brkic et al. 2019) and the *PVSys-tems* (Villalva, Gazoli, and Ruppert Filho 2009). The former is based on the single-diode model and contains various examples and validation data. It is also based on manufacturer data only but neglects the effect of different mounting types, which affect the cell temperature. In addition, the latter library is also based on the single-diode approach and applies a numerical solution method to obtain the 5 unknown parameters (Villalva, Gazoli, and Ruppert Filho 2009). However, according to Brkic et al. (2019), the library is missing a parameterization support for the parallel and serial resistances. In addition, simulation results for the open-circuit voltage do not necessarily match the points provided in the data sheets (Brkic et al. 2019). As in the case of the *PhotoVoltaics* library, the mounting's effect on the cell temperature and, hence, the module's efficiency is not included. To summarize, most of the implemented models rely on the same physical assumptions, i.e., the single-diode approach. However, literature is currently missing a detailed comparison

of the single- and the two-diodes approach. Furthermore, the mounting's effect on the cell temperature has not yet been implemented in any of the analysed models. Finally, an implementation in the *IBPSA* library facilitates the use in the derivative libraries due to consistent interfaces and parameterization schemes.

## 3 Methodology

The following section gives an overview of the model implementation. In the last section, we describe the rooftop system in Berlin that is used for the validation.

### 3.1 Model implementation

#### 3.1.1 Basic model structure

Figure 3 presents the basic model structure. The two model formulations both extend the `PartialPVSystem` model. The weather data, i.e., the dry bulb temperature, the wind velocity, and the global irradiation on the tilted surface are given by existing models of the package `IBPSA.BoundaryConditions`. The `PartialPVSystem` includes three replaceable models, namely the `PartialPVElectrical`, the `PartialPVThermal`, and the `PartialPVOptical`. The `PartialPVElectrical` model calculates the I-V characteristic. The single- and two-diodes modeling approach are implemented. The `PartialPVThermal` model computes the cell temperature, taking into account how the PV mounting type affects the cell temperature due to the wind velocity. The `PartialPVOptical` model calculates the PV-material-specific absorption ratio of the module, which is an input to the thermal and the electrical model. The overall model inputs comprise weather information such as the zenith angle, the incidence angle, the diffuse horizontal irradiation, the irradiation on the tilted surface, the irradiation on the horizontal surface, the dry bulb temperature as well as the wind velocity via real inputs. In addition, the tilt and azimuth angle can be manipulated by real inputs if not used as parameters. The model outputs the DC power using a real output connector. The current and voltage as well as the cell temperature are additional model variables.

#### 3.1.2 Single-diode modeling approach

One of the implemented electrical partial models follows the single-diode approach as described in subsection 3.1.2. The model is based on five unknown parameters that need to be estimated. To determine these parameters, two approaches exist: an iterative, numerical solution method and an analytical one. Since the numerical approach is computationally less efficient, and to avoid users having to provide start values for the iteration variables, the implemented model uses the analytical approach. Even though it is less accurate, it does not suffer from initialization problems and is robust (Bai et al. 2014). We implement the approach presented by Bai et al. (2014). It is based on the approximation of the Lambert W func-

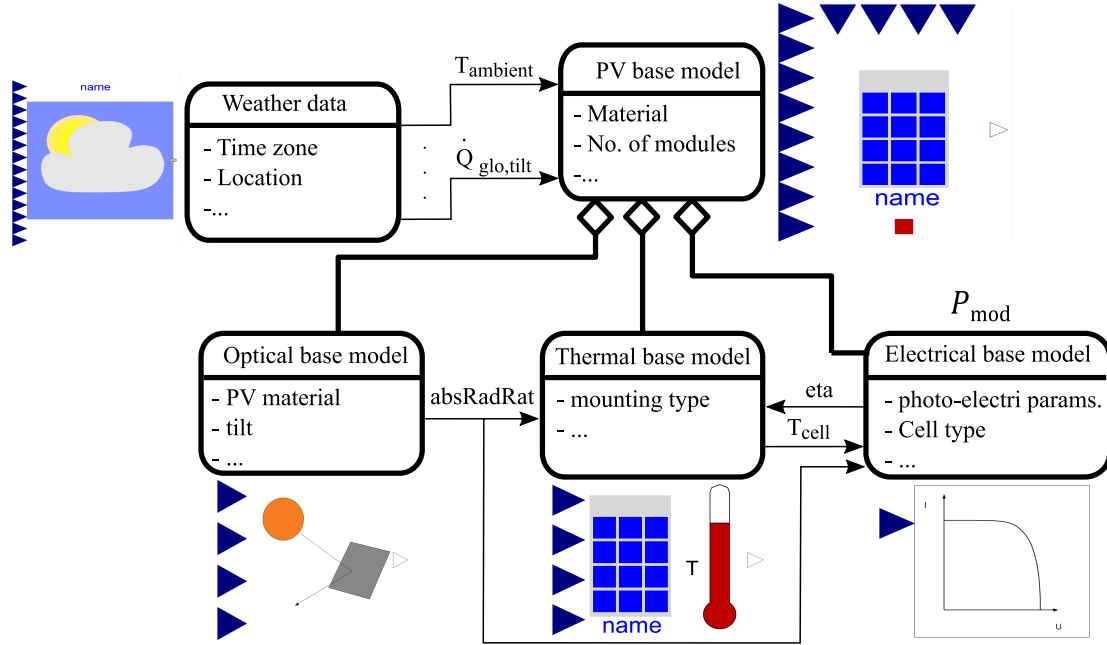


**Figure 3.** Basic model structure with partial models, main interfaces, and parameters. For simplicity, only the main parameters and variables are displayed.

tion and uses simplifications to derive an explicit formulation of the I-V characteristic based on manufacturer data, only. In addition, it provides explicit formulations for the initialization of the five unknown parameters. For more details on the initialization method, we refer to Bai et al. (2014). The current and voltage at the MPP is deduced as described in Bai et al. (2014),

$$I_{mp} = I_{ph} \left(1 - \frac{1}{w}\right) - a \frac{(w-1)}{R_{sh}} \quad (12)$$

$$U_{mp} = a(w-1) - R_s I_{mp}, \quad (13)$$

where  $w$  is the wind velocity. Bai et al. (2014) do not consider any temperature- or irradiation-dependence of the parameters. Since the presented model aims to consider these dependencies, we assume for the operating conditions equations based on De Soto, Klein, and Beckman (2006) and Messenger and Abtahi (2017),

$$\frac{a}{a_0} = \frac{T_{cell}}{T_{cell,0}}, \quad (14)$$

$$I_{ph} = \frac{H_{tilt}}{H_{tilt,0}} (I_{ph} + \mu_{I,K} (T_{cell} - T_{cell,0})), \quad (15)$$

$$\frac{I_s}{I_{s,0}} = \left(\frac{T_{cell}}{T_{cell,0}}\right)^3 e^{\left(\frac{E_{g,0}}{kT_{cell,0}} - \frac{E_g}{kT_{cell}}\right)}, \quad (16)$$

$$\frac{E_g}{E_{g,0}} = 1 - C(T_{cell} - T_{cell,0}). \quad (17)$$

We assume that the parallel resistance  $R_{sh}$  is temperature invariant, but that it depends on irradiation, and we assume

the serial resistance to be constant (De Soto, Klein, and Beckman 2006). Therefore,

$$\frac{R_{sh}}{R_{sh,0}} = \frac{H_0}{H}, \quad (18)$$

$$R_s = R_{s,0}. \quad (19)$$

This approach is purely based on manufacturer data and is, therefore, simple to parameterize. At this point, we highlight that even though the unknown quantities are called parameters in the scientific literature, they are variables within the models. The proposed method includes pre-defined initialization values for those variables and calculates their values during operation using (14) to (19). Despite its simplicity, the single-diode approach is based on strong assumptions regarding the behavior of the parallel and serial resistance. In this contrast, the two-diodes approach described in the next section provides a more accurate representation.

### 3.1.3 Two-diodes modeling approach

We implemented the two-diodes model as

$$0 = I_{ph} - I_{S1} \left( e^{\frac{U_{mp} + I_{mp} R_s}{n_{ser} U_t}} - 1 \right) - I_{S2} \left( e^{\frac{U_{mp} + I_{mp} R_s}{2U_t}} - 1 \right) - \frac{U_{mp}}{n_{ser}} + \frac{I_{mp} R_s}{n_{par} R_{sh}} \frac{I_{mp}}{n_{par}}, \quad (20)$$

$$0 = \frac{I_{mp}}{n_{par}} - \lambda \frac{I_{Sat1}}{U_t} e^{\frac{U_{mp} + I_{mp} R_s}{n_{ser} U_t}} + \frac{I_{Sat2}}{2U_t} e^{\frac{U_{mp} + I_{mp} R_s}{2U_t}} + \frac{1}{R_{sh}}, \quad (21)$$

and

$$0 = \frac{U_{mp}}{n_{ser}} - \lambda \frac{R_s I_{S1}}{U_t} e^{\frac{U_{mp} + (\frac{I_{mp}}{n_{par}}) R_s}{U_t}} + \frac{R_s I_{S2}}{2U_t} e^{\frac{U_{mp} + (\frac{I_{mp}}{n_{par}}) R_s}{2U_t}} + \frac{R_s}{R_{sh} + I}, \quad (22)$$

where the module voltage  $U_{mp}$  and module current  $I_{mp}$  are unknowns. The calculation of the current  $I_{mp}$  and voltage  $U_{mp}$  in the MPP uses the method of Lagrange multipliers to find the maximum of power  $P_{mp} = I_{mp} U_{mp}$ . This leads to a system of three equations for the three unknowns  $I_{mp}$ ,  $U_{mp}$  and  $\lambda$ .

With the two-diodes model, the electrical behavior of a PV module can be represented more accurately due to the second diode in the equivalent circuit. The drawback is that the six parameters cannot be derived from manufacturer data, as is the case with the single-diode model, but must be determined using optimization. For parameter fitting, we use GenOpt (Wetter 2009).

### 3.1.4 Thermal modeling approach

To calculate the cell temperature, we implemented three different thermal modeling approaches. These are implemented using replaceable classes of the thermal base model, allowing the user to select the modeling approach that corresponds best to the mounting situation. In addition to the physics-based model for the open rack installation, we also integrated the empirical models of King, Boyson, and Kratochvill (2005). They reflect a mounting close to ground and in contact with ground, respectively. King, Boyson, and Kratochvill (2005) found their cell temperature calculation to be applicable for different cell types.

## 3.2 Preliminary studies

Both modeling approaches have been partially validated in preliminary studies. The single-diode modeling approach combined with the implemented thermal models has been validated in Maier, Kratz, et al. (2021) using measurement data from the National Institute of Standards and Technology (NIST). The underlying model was integrated in the *AixLib* library (Maier, Jansen, et al. 2023). The measurement data was taken from two different arrays consisting of mono-SI wafer-cell-based modules. We extend the existing work by including an analysis of the thermal model and focusing on thin-film CIGS modules. The two-diodes model has been developed and presented in Pruthviraj Balekai (2018) and implemented in the *BuildingSystems* library (Nytsch-Geusen, Huber, Ljubijankic, et al. 2013). This work enhances the model by implementing it in a modular model structure that forms the basis of the single- and two-diodes modeling approach. In addition, the thermal model has been replaced.

## 3.3 Validation data

The measured values for the validation of the newly developed single-diode and two-diodes models were obtained

using the monitoring system of the rooftop experimental building<sup>1</sup> as shown in Figure 4), which is located on the university campus in Berlin-Charlottenburg. A total of 84 thin-film PV modules (type Solibro SL2 CIGS 110-120<sup>2</sup>) with a total power of 9.24 kW<sub>peak</sub> are installed on the roof of the building on two movable single-axis tracking facade elements.



**Figure 4.** Rooftop building with roof and facade mounted photovoltaic system in Berlin (Germany).

These modules are monitored separately in 42 groups, each with 2 interconnected PV modules using the SolarEdge (SolarEdge 2006) monitoring platform. For the validation, a non-movable, rarely shaded module group on the roof was selected, which has a slight inclination of 2° and is oriented 27.5° to the west. The following variables were recorded in a time interval of 5 min during the monitoring process for this module:

- Module temperature (using a digital sensor on the back of the module),
- total horizontal radiation (using KIPP and Zonen SP Lite Pyranometer),
- wind speed and direction and outside air temperature, using the Netatmo (Netatmo 2011) weather station, and
- electric power per module group (4 x 120 W<sub>peak</sub> and 2 x 115 W<sub>peak</sub>) using the monitoring system as shown in Figure 5.

The data from the Netatmo weather station are extracted using a Python-based data collector which then feeds it to the InfluxDB data base for further processing. The module temperature and total horizontal radiation is collected individually using NodeMCU microcontroller and then fed wireless to InfluxDB via MQTT.

<sup>1</sup><http://www.solar-rooftop.de>

<sup>2</sup>[https://hanergy.eu/wp-content/uploads/2015/08/Solibro\\_data-sheet\\_SL2-F-module\\_G1-4\\_100-110-120-125\\_EN.pdf](https://hanergy.eu/wp-content/uploads/2015/08/Solibro_data-sheet_SL2-F-module_G1-4_100-110-120-125_EN.pdf)



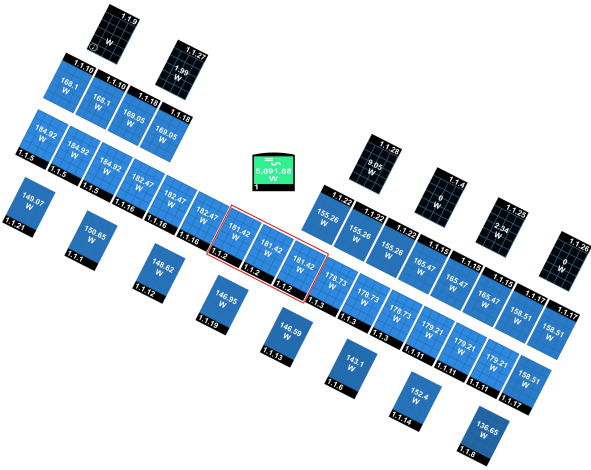


**Figure 5.** Layout of the PV system with 84 PV modules and generated electricity on April 30<sup>th</sup>, 2023 (and the selected PV system marked in red rectangle).

## 4 Results

This section first describes the results from the model implementation and continues by discussing the validation.

### 4.1 Model application

#### 4.1.1 Single-diode model application

The parameters of the single-diode model is based on the manufacturer data, only. The following five parameters were used to parameterize the 115 Wp (and 120 Wp module, respectively):  $I_{sc,0} = 1.69$  A (1.71 A),  $V_{oc,0} = 101.2$  V (102.3 V),  $\eta_{a0} = 0.122$  (0.128),  $\alpha_{Isc,0} = 0.01$  %/K,  $\beta_{Voc,0} = -0.27$  %/K,  $\gamma_{PMPP,0} = -0.32$  %/K, and  $P_{MPP,0} = 115$  W.

#### 4.1.2 Two-diodes model application

To determine the parameters of the two-diodes model, a set of U-I characteristics curves for different cell temperatures of the module type Solibro SL2 CIGS 110 were used. We note that we only had access to data for the modules with a peak power of 110 W. However, the target system comprises four modules with a peak power of 115 W and 120 W. Consequently, we cannot directly compare measured with simulated data for the two-diodes model. To still validate the plausibility of the two-diodes model, a second validation set is generated. For the second validation set, the single- and the two-diodes models are both parameterized with 110 Wp modules. This serves as a plausibility check for the two-diodes model. Note, however, that the lack of measurement data for the 110 Wp modules precludes an assessment of the accuracy of the single- vs. two-diodes model.

To obtain the best possible combination of the six model parameters using optimization, a cost function was defined. This function calculates the squares of the difference between the calculated module current with

the two-diodes model and the value from the manufacturer curve for 20 different voltage values along the U-I curve. We used the Hooke-Jeeves algorithm from GenOpt, which yields the following parameters values:  $R_s = 0.027484527$   $\Omega$ ,  $R_{sh} = 500.0$   $\Omega$ ,  $c_1 = 0.0011962052$ ,  $c_2 = 0.001542755$ ,  $c_{S1} = 9.490919$ , and  $c_{S2} = 0.007634368$ .

### 4.2 Model validation and plausibility check

The validation and plausibility check comprises three aspects: (i) the validation of the single-diode model (115 Wp and 120 Wp) using the measurement data (see Section 4.2.1), (ii) the plausibility check of the two-diodes model using the single-diode model (110 Wp) simulation results (see Section 4.2.2), and (iii) the cell temperature validation (see Section 4.2.3). The validation period is from July 27<sup>th</sup> until August 9<sup>th</sup>, i.e., it covers 12 d. To evaluate the cell temperature approaches, an exemplary day from the spring period was added.

#### 4.2.1 Validation of the single-diode model

Figure 6 depicts the curves of the simulated and measured DC power output of the six modules for the single-diode model. A comparison of the simulated and the measured DC power for the whole validation period yields an  $R^2$  value of 0.86 and a mean absolute error of 16.6 W. This is rated as a high accuracy. The measurement data contains days with low, medium, and high irradiation, which confirms high model accuracy for different operating conditions. To better understand the data, Figure 7 picks an exemplary day. We select July 30<sup>th</sup> as an exemplary day because it covers both high and low irradiation periods during one day. The figure shows the simulated and measured DC output power of the modules on the top and the global horizontal irradiation at the bottom. We observe that the simulated and measured DC power generally follow the trend of the global irradiation, as expected. However, at around 3 pm, the measurements show a DC power peak, while the simulation and irradiation data do not. A potential explanation is that the irradiation sensor might detect shading while the observed modules do not. Other possible explanations include imperfect calibration of the irradiation sensor or measurement errors. However, since this behaviors is only observed for a negligible amount of time, the overall measurement data quality is rated high.

#### 4.2.2 Plausibility check for the two-diodes model

Since the measurement data do not cover 110 Wp modules, the two-diodes model is compared to the simulation data of the single-diode model. For this plausibility check, the single-diode models are parameterized based on the manufacturer data of the 110 Wp modules. Figure 8 illustrates the simulated DC powers of both modeling approaches for July 30<sup>th</sup>. When comparing the simulated outputs, it becomes evident that they are almost identical. The comparison for the whole validation period of 12 d yields an  $R^2$  value of 0.99 and a mean absolute error of 5.5 W. This is a high accuracy and it shows that both models yield similar DC power outputs.

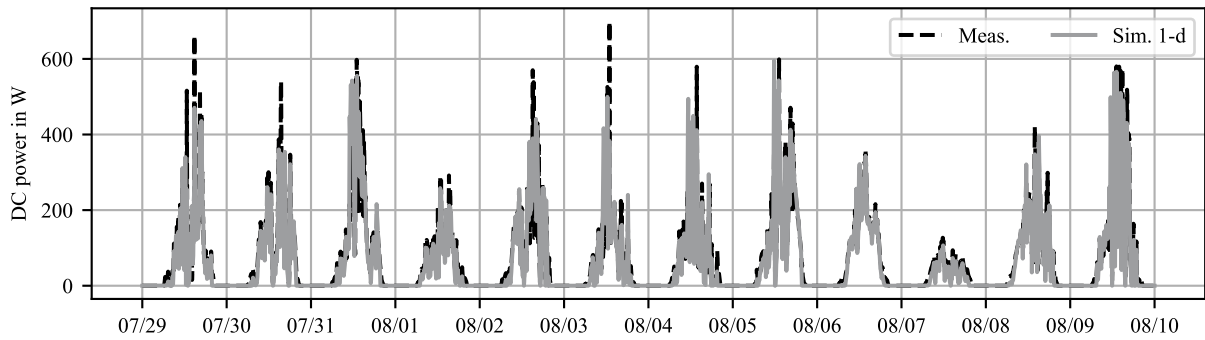


**Figure 6.** Comparison of measured and simulated DC power output for the validation period for the single-diode approach.

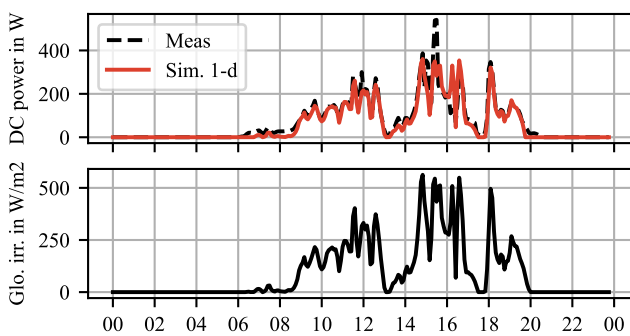


**Figure 7.** July 30<sup>th</sup> as an exemplary day to demonstrate the accuracy of the single-diode model.

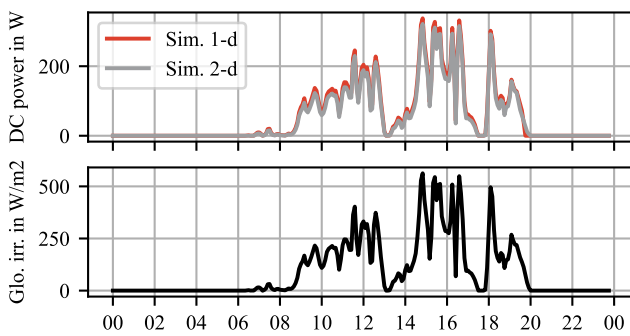


**Figure 8.** July 30<sup>th</sup> as an exemplary day to compare the single- and two-diodes model outputs.

### 4.2.3 Cell temperature validation

In addition to the DC power, we also validated the cell temperature model. Figure 9 shows the curves of the measured cell temperature, the ambient temperature, and the simulated cell temperature for the three modeling approaches (“open rack”, “close to ground”, and “in contact with ground”), as discussed in Section 3.1.4, for a spring (left) and a summer day (right). The thermal model corresponding to the mounting of the use case is “close to ground”, the other modeling approaches are added to the figure for plausibility check. While for the spring day, the

thermal model corresponding to the mounting type “close to ground” best predicts the cell temperature, the mounting type “open rack” results in the highest accuracy for the summer day. When taking the  $R^2$  as a KPI, the following values are realized for the spring (and summer) day, respectively: “close to ground”: 0.81 (0.3), “open rack”: 0.7 (0.75), and “in contact with ground”: 0.68 (-0.01). The cell temperature calculations are, among other influences, based on the wind velocity and the ambient temperature. On the summer day, the ambient temperature is higher while the wind velocity is lower. The thermal models seem to overestimate this combined influence on the temperature leading to an overestimation of the temperature. In addition, we observe that the model overestimates the cell temperature during the night time. We find that the assumption of the cell temperature reaching the dry bulb temperature during no-irradiation periods is incorrect. The PV modules experiences radiative heat transfer with the sky leading to lower cell temperatures than the dry bulb temperatures during no-irradiation periods. However, the night time is not relevant for PV system evaluation since no DC power is generated.

Finally, we discuss the CPU time of the model. Both models result in a similar set of equations. While the single-diode model has 544 equations, the two-diodes model results in 534. To compare the CPU times, we simulated both models for the validation period 10 times and took the median of the CPU times. The simulations were done on a Lenovo L480 with an Intel Core i5-8250U CPU and 1.60 GHz. The operating system is Windows 10 and Dymola 2023 was used as simulation environment. Two-diodes model results in average CPU times of 0.19 s and single-diode of 0.2 s. Consequently, we rate the models’ simulation speed as sufficiently fast for most applications.

## 5 Limitations

The validations show high accuracy of DC power output for the single-diode model for the thin-film CIGS module. Due to missing measurement data for the 110 Wp modules, we cannot directly validate the two-diodes model making a general comparison between both modeling techniques difficult. The cell temperature validation



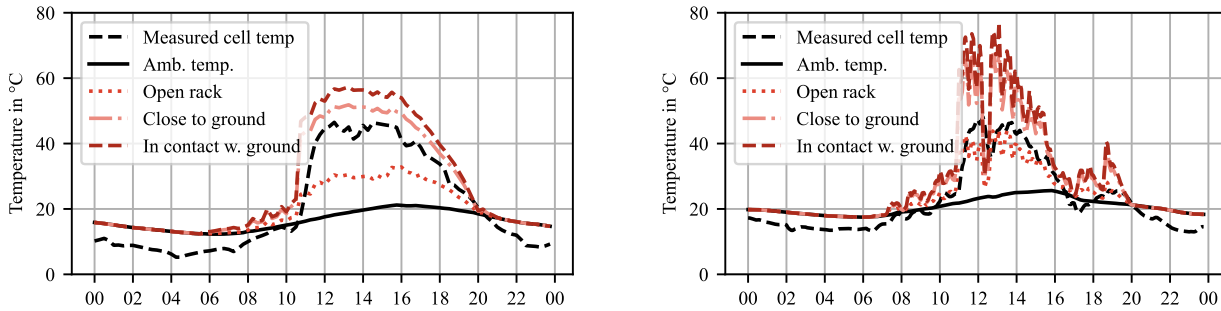


**Figure 9.** Comparison of measured and simulated cell temperature for a spring day (left) and a summer day (right). Both the two- and single-diode model use the same cell temperature model.

shows that the cell temperature model overestimates the actual temperature, especially during summer days. However, the cell temperature computations only have a small effect on the computed DC power due to small temperature coefficients of the modules ( $\alpha_{I_{sc},0} = 0.01\%/K$  and  $\beta_{V_{oc},0} = -0.27\%/K$ ). Uncertainty may be introduced by the irradiation sensor not capturing all shading effects of the six modules. This might lead to an overestimation of the power output at certain points as shown in Figure 7.

We focus the validation on the summer period. The validation should be extended to account for colder days and days with almost no direct irradiation. This is explained by the advantage of thin-film CIGS modules that benefit from diffuse radiation. In addition, the cell temperature model validation should be extended to a very cold winter day to capture all relevant effects and better understand how to correctly select an appropriate thermal model. Moreover, the presented models were not yet validated regarding their accuracy in current and voltage estimation. Even though it is possible to model each module separately, we modelled the PV array as one system and neglected the detailed electrical connections between the modules. For such a detailed analysis, we expect the two-diodes model to outperform the simplified single-diode model.

## 6 Conclusions

We presented a new open-source Modelica model of a PV system that is implemented in the Modelica IBPSA Library. The model includes two typical modeling approaches for the electrical characteristics of PV modules, a single- and a two-diodes approach. To validate the model, real measurement data from a rooftop building in Berlin, Germany, was used. The validated PV modules are thin-film CIGS cells. The comparison is done for a validation period in July and the DC power output and cell temperature are analysed. The investigation reveals that the single-diode model captures the PV DC power output well (see Figure 6) and that the two-diodes model estimates similar DC power outputs (see Figure 8). However, we could not evaluate which modeling technique is favorable since proper measurement data for the two-diodes model were

not available, and we therefore only verified its accuracy based on the single-diode model.

The mounting situation of the measured system corresponds to an installation close to ground. The simulation results show that this approach does not necessarily lead to the best cell temperature estimation (see Figure 9). For the regarded spring day, the cell temperature model for the intended mounting type results in the highest accuracy, while for the summer day, the cell temperature model corresponding to an installation with open rack yields the highest accuracy. The thin-film modules are characterized by small temperature coefficients and, hence, their performance decline with increasing cell temperatures is small.

## 7 Future work

The present paper shows the comparison and validation for a thin-film CIGS PV module. Even though, the single-diode model has been validated before based on mono-Si modules, literature is still lacking a comparison of the two presented modeling approaches for a wider range of typical configurations. These configurations include mono- and poly-Si wafer cells for different setups (i.e., tilts and mountings) as well as orientations and locations. Validation data of different mounting situations could also be used to further validate the cell temperature calculations implemented in the thermal model. Furthermore, our validation does not include a detailed current and voltage analysis due to missing data. Moreover, the validation only focuses on 12 days in July. Even though the validation period was carefully selected to cover different irradiation situations, validation in other seasons would be beneficial.

## 8 Data availability

The validations were done with the model that is available in the Modelica IBPSA Library and can be found at <https://github.com/ibpsa/modelica-ibpsa/pull/1766><sup>3</sup>. The measurement data is available in the corresponding IBPSA resources folder and obtained from the UdK Berlin.

<sup>3</sup>The corresponding commit hash is 6e263f8cfa1ea65c0f4f91b610f205ece11e8a51.

## Acknowledgements

We gratefully acknowledge the financial support by the Federal Ministry for Economic Affairs and Climate Action (BMWK), promotional reference 03EN3026C. This research was supported by the Assistant Secretary for Energy Efficiency and Renewable Energy, Office of Building Technologies of the U.S. Department of Energy, under Contract No. DE-AC02-05CH11231. The described research was also conducted within the project “Eneff: HCBC 1. Umsetzungsphase HochschulCampus Berlin-Charlottenburg” and funded by the Federal Ministry for BMWK, reference 03ET1632B. This work emerged from the IBPSA Project 1, an international project conducted under the umbrella of the IBPSA. Project 1 has developed and demonstrated a BIM/GIS and Modelica Framework for building and community energy system design and operation.

## References

- 2022 *Global status report for buildings and construction: Towards a zero-emissions, efficient and resilient buildings and construction sector* (2022). Nairobi. ISBN: 978-92-807-3984-8.
- Bai, Jianbo et al. (2014). “Development of a new compound method to extract the five parameters of PV modules”. In: *Energy Conversion and Management* 79, pp. 294–303.
- Batzelis, Efstratios (2019). “Non-iterative methods for the extraction of the single-diode model parameters of photovoltaic modules: A review and comparative assessment”. In: *Energies* 12.3, p. 358.
- Batzelis, Efstratios I and Stavros A Papathanassiou (2015). “A method for the analytical extraction of the single-diode PV model parameters”. In: *IEEE Transactions on Sustainable Energy* 7.2, pp. 504–512.
- Brkic, Jovan et al. (2019). “Open Source PhotoVoltaics Library for Systemic Investigations”. In: *Proceedings of the 13th International Modelica Conference, Regensburg, Germany, March 4–6, 2019*. Linköping Electronic Conference Proceedings. Linköping University Electronic Press, pp. 41–50. DOI: 10.3384/ecp1915741.
- De Soto, Widaly, Sanford A Klein, and William A Beckman (2006). “Improvement and validation of a model for photovoltaic array performance”. In: *Solar energy* 80.1, pp. 78–88.
- Duffie, John A and William A Beckman (2013). *Solar engineering of thermal processes*. John Wiley & Sons.
- Jakhrani, Abdul Qayoom et al. (2011). “Determination and comparison of different photovoltaic module temperature models for Kuching, Sarawak”. In: *2011 IEEE Conference on Clean Energy and Technology (CET)*. IEEE, pp. 231–236.
- Jorissen, Filip et al. (2018). “Implementation and Verification of the IDEAS Building Energy Simulation Library”. In: *Journal of Building Performance Simulation* 11 (6), pp. 669–688. DOI: 10.1080/19401493.2018.1428361.
- King, David L., William E. Boyson, and J. A. Kratochvill (2005). “SANDIA REPORT SAND 2004-3535 Unlimited Release Printed December 2004 Photovoltaic Array Performance Model”. In.
- Maier, Laura, David Jansen, et al. (2023). “AixLib: an open-source Modelica library for compound building energy systems from component to district level with automated quality management”. In: *Journal of Building Performance Simulation* 0.0, pp. 1–24. DOI: 10.1080/19401493.2023.2250521. eprint: <https://doi.org/10.1080/19401493.2023.2250521>. URL: <https://doi.org/10.1080/19401493.2023.2250521>.
- Maier, Laura, Michael Kratz, et al. (2021). “Open-source photovoltaic model for early building planning processes: Modeling, application and validation”. In: *Building Simulation 2021*. Vol. 17. IBPSA, pp. 2315–2316.
- Messenger, Roger A and Amir Abtahi (2017). *Photovoltaic systems engineering*. CRC press.
- Netatmo (2011). accessed June 08, 2023. <https://www.netatmo.com/>.
- Nytsch-Geusen, Christoph, Jörg Huber, Manuel Ljubijankic, et al. (2013). “Modelica BuildingSystems – eine Modellbibliothek zur Simulation komplexer energietechnischer Gebäudesysteme”. In: *Bauphysik* 35.1, pp. 21–29. ISSN: 01715445. DOI: 10.1002/bapi.201310045.
- Nytsch-Geusen, Christoph, Jörg Huber, and Yue Nie (2013). “Simulation-based design of PV cooling systems for residential buildings in hot and dry climates”. In: *13th International Conference of the International Building Performance Simulation Association*.
- Pruthviraj Balekai, Pruthviraj (2018). “Energy performance analysis of single axis tracking PV system for the Rooftop Building based on Modelica and openHAB”. Master thesis. Berlin, Germany: Technische Universität Berlin.
- Romary, Florian et al. (2011). “Thermal modelling to analyze the effect of cell temperature on PV modules energy efficiency”. In: *Proceedings of the 2011 14th European Conference on Power Electronics and Applications*. IEEE, pp. 1–9.
- Sellner, Stefan et al. (2012). “Understanding PV module performance: Further validation of the novel loss factors model and its extension to AC arrays”. In: *27th European Photovoltaic Solar Energy Conference and Exhibition*, pp. 3199–3204.
- SolarEdge (2006). Accessed June 08, 2023. <https://www.solaredge.com/>.
- Stein, Joshua et al. (2013). *Outdoor PV performance evaluation of three different models: single-diode SAPM and loss factor model*. Tech. rep. Sandia National Lab.(SNL-NM), Albuquerque, NM (United States).
- Sutterlueti, J et al. (2008). “Characterising PV modules under outdoor conditions: what’s most important for energy yield”. In: *Channels* 48.24, p. 24.
- Villalva, Marcelo Gradella, Jonas Rafael Gazoli, and Ernesto Ruppert Filho (2009). “Comprehensive approach to modeling and simulation of photovoltaic arrays”. In: *IEEE Transactions on power electronics* 24.5, pp. 1198–1208.
- Wetter, Michael (2009-05). *GenOpt, Generic Optimization Program, User Manual, Version 3.0.0*. Tech. rep. LBNL-2077E. Berkeley, CA, USA: Lawrence Berkeley National Laboratory.
- Wetter, Michael, Christoph van Treeck, et al. (2019-09). *IBPSA Project 1: BIM/GIS and Modelica framework for building and community energy system design and operation – ongoing developments, lessons learned and challenges*. DOI: 10.1088/1755-1315/323/1/012114. URL: <https://doi.org/10.1088/1755-1315/323/1/012114>.
- Wetter, Michael, Wangda Zuo, et al. (2014). “Modelica Buildings library”. In: *Journal of Building Performance Simulation* 7.4, pp. 253–270. ISSN: 1940-1493. DOI: 10.1080/19401493.2013.765506.